**Title**
DYNAMICS OF THE C+ -H2 REACTION



**Authors**
Mahan, Bruce H.
Sloane, Thompson M.

**Publication Date**
1973-08-01

Submitted to
J. Chem. Phys.

LBL-1869
Preprint

# DYNAMICS OF THE $C^+$-$H_2$ REACTION

Bruce H. Mahan and Thompson M. Sloane

August 1973

Prepared for the U. S. Atomic Energy Commission
under Contract W-7405-ENG-48



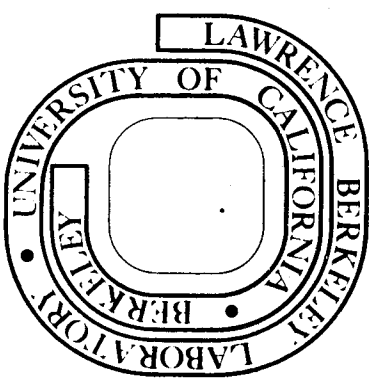

## DISCLAIMER

# Dynamics of the $C^+$-$H_2$ Reaction

Bruce H. Mahan and Thompson M. Sloane
Department of Chemistry, and Inorganic Materials
Research Division of the Lawrence Berkeley Laboratory,
University of California, Berkeley 94720

The reaction of $C^+(H_2,H)CH^+$ and its isotopic variants have been investigated by measuring the velocity vector distribution of product ions formed when a collimated, energy selected beam of $C^+(^2P_{\frac{1}{2}})$ impinges on a target gas. At relative energies below 4 eV, the reaction product velocity distribution shows a high, but not perfect, degree of symmetry in the barycentric system. The non-reactively scattered $C^+$ shows a very inelastic component in addition to elastic features. The form of the distributions suggests that in many collisions, the system passes through configurations in which all three atoms interact strongly for times which are of the order of one rotational period. At higher relative energies, the product distributions are consistent with a direct interaction mechanism, but indications of strong three-body interactions remain. The behavior is consistent with the electronic state correlation diagram for the system, which shows that the deep (4 eV) potential well of symmetric $CH_2^+$ is accessible to the reactants and products.

A major goal of the study of molecular collisions is to learn how to anticipate the dynamics of an elementary reaction without engaging in a major numerical calculation of the potential energy surfaces of the system. If, for example, one could reliably identify the systems which have surfaces that lead to strongly coupled collision complexes, then much of the interesting dynamical information for these systems could be predicted by statistical or phase space theories. To be able to make such identifications, one must learn how to deduce the salient properties of potential energy hypersurfaces by examining and correlating the electronic properties of the reactants, products and intermediate species. Demonstrations of the utility of electronic state and orbital correlation diagrams in guiding the interpretation of small molecule reaction phenomena have been given by Herschbach and coworkers,[1,2] Tully et al,[3] Friedman et al,[4] Donovan and Hussain,[5] and Mahan and coworkers.[6,7]

Ion-molecule reactions can present particularly challenging problems to the application of correlation diagram techniques. The systems involved are frequently of the open-shell type, and thus there may be several surfaces which lie within a few eV of the ground state surface. The situation is further complicated by the fact that in addition to surfaces generated from combinations of the various states of reactants $A^+$ and BC, there is a manifold of surfaces which arise from the states of $A + BC^+$. Since the ionization

energies of most atoms and molecules differ by less than 5 eV, these two manifolds of surfaces are apt to be interwoven in a potentially complicated manner. Thus, the dynamics of a given ion-molecule reaction may be profoundly influenced by intersections and avoided crossings of the potential hypersurfaces.[4] Indeed, this seems to be the case even for the simplest ion-molecule reactions.[8] As part of a program intended to elucidate the relation between the collision dynamics and the electronic properties of ion-molecule systems having few electrons, we have investigated the reactive and non-reactive scattering of $C^+$ by $H_2$, HD, and $D_2$, and report the results here.

The $C^+(D_2,D)CD^+$ reaction was first investigated by Maier,[9] who used a fixed angle tandem mass spectrometer to determine the energy dependence of the total reaction cross section. Koski and coworkers[10] also used a tandem mass spectrometer to determine the reaction threshold energy and the total reaction cross section as a function of relative energy in the range from 0.5 to 20 eV. In addition, Iden, Liardon, and Koski[11,12] have reported studies of the energy and angular distributions of the product of the $C^+(D_2,D)CD^+$ reaction for several initial relative energies. Henchman et al[13] recently measured the energy dependence of the total cross section for the reaction of $C^+$ with $H_2$ and $D_2$, and also determined the $CH^+/CD^+$ ratio as a function of energy for the reaction of $C^+$ with HD.

The product angular distributions measured by Iden, Liardon, and Koski[12] show at low ($\lesssim$ 4.4 eV) relative energies, considerable symmetry about the $\pm$ 90° axis in the center of mass system. They took this to indicate that the reaction proceeds through a persistent collision complex which has a lifetime in excess of the rotational period, approximately $10^{-12}$ sec. A long-lived collision complex would indeed give such highly symmetric distributions, but these scattering patterns can also be produced by direct interaction processes.[14,15] The interpretation of Iden, Liardon, and Koski[12] was questioned by Mahan[6] on the grounds that a simple triatomic molecule with 3-4 eV energy in excess of that needed to dissociate would not be expected to have a lifetime of the several rotational periods needed to produce highly symmetric product velocity distributions. In addition, since the orbital configuration of the reactants is different from that of the ground state of the intermediate $CH_2^+$, it seemed to be questionable whether or not the deep potential well necessary for a persistent complex was accessible to the reactants. Moreover, the $CH^+/CD^+$ ratios measured by Henchman *et al*[13] differ in size and energy dependence from the predictions calculated by Truhlar,[16] who used a phase space theory which would be expected to apply to a reaction proceeding through a persistent complex. Thus, other experiments which might elucidate the mechanism of this reaction seemed to be called for.

## Experimental

The instrument used in this work has been described in detail previously.[17] It consists of a magnetic mass spectrometer for preparation of a collimated beam of primary ions of known energy, a scattering cell to contain the target gas, and an ion detection train made up of an electrostatic energy analyzer, a quadrupole mass spectrometer, and an ion counter. The detector components and the exit aperture of the scattering cell are mounted on a rotatable lid, which permits the intensity of scattered ions to be measured at various angles and energies.

Primary ions were extracted from a microwave discharge through a carbon dioxide-helium mixture. The intensity of the $C^+$ was less than, but comparable to, the intensity of $CO_2^+$ issuing from the discharge. The direct production of $C^+$ by electron impact on neutral CO or $CO_2$ requires electron energies of 20 eV or more. Microwave discharges operated at the power levels and pressures we employed have approximately thermal electron energy distributions corresponding to temperatures of 4-5 eV. Thus there are very few electrons with enough energy to produce directly ion products of high appearance potential. Indeed, in previous publications[7,18] we have shown that metastable excited ions which require electron energies in excess of 13-15 eV are not produced in detectable amounts by microwave discharges. Consequently, it seems highly likely that the $C^+$

in our source is produced by ionization of carbon atoms which are themselves formed by the dissociation of $CO_2$ and CO by low energy electron impact. Because of the low electron temperature in the discharge and the fact that the first metastable excited state ($^4P$) of $C^+$ lies 5.32 eV above the ground state, it seemed highly probable that the $C^+$ in our collimated beam was almost entirely in the ground electronic state, $^2P_{\frac{1}{2}}$. This was confirmed by beam attenuation measurements of the type described by Turner et al.[19]

Our experimental results are presented in the form of contour maps of the specific intensity $\bar{I}(\theta,u)$, the intensity of ions per unit velocity space volume normalized to unit beam strength, scattering gas density, and collision volume. A polar coordinate system is used, with the radial coordinate u representing the speed of the ion relative to the center-of-mass of the target-projectile system, and the angular coordinate $\theta$ measured with respect to the original direction of the projectile ion beam. The specific intensity is normalized such that

$$\bar{\sigma} = 2\pi \int_0^{\pi} \sin\theta d\theta \int_0^{\pi} u^2 \bar{I}(\theta,u) du$$

is always proportional to the true cross section $\sigma$. Each contour map is generated from 10-20 scans of the laboratory energy and angular distributions, in each of which 10-20 intensity measurements are made.

## Results and Discussion

The energetics of the reaction

$$C^+(^2P_{\frac{1}{2}}) + H_2\ (^1\Sigma) \rightarrow CH^+\ (^1\Sigma) + H(^2S) \qquad (1)$$

can be the source of some confusion. Use of the heats of formation tabulated by Franklin et al[20] leads to the conclusion that the reaction is 0.8 eV endoergic. However, the $\Delta H_f(CH^+)$ tabulated by Franklin et al seems to be based on an early value of 11.13 eV for the ionization energy of CH. The more recent value[21] of 10.64 eV leads to a dissociation energy $D_0(CH^+)$ equal to 4.1 eV, and a $\Delta H$ of +0.4 eV for reaction 1. This value is consistent with the threshold energy for the reaction determined by Koski et al,[10] and is adopted here.

The translational exoergicity Q of a reaction is given by

$$Q = E_{rel}' - E_{rel} = -\Delta E_0^0 - U' + U$$

where $E_{rel}$ is the initial relative energy, U is the internal energy of the reactants, and the $E_{rel}'$ and U' are the corresponding quantities for the products. Assuming U = 0, and recognizing that for $CH^+(^1\Sigma)$, U' must lie between zero and the dissociation energy of $CH^+$ to $C^+$ and H, we get

$$-4.5 \leqslant Q \leqslant -0.4 \text{ eV} \qquad (2)$$

For reaction to form any other electronically excited state of $CH^+$ which dissociates to $C^+$ and H, the upper limit of Q becomes more negative by the minimum excitation energy of

the state involved, and the lower limit remains the same. If a state of $CH^+$ is formed that dissociates to $C(^3P)$ and $H^+$, the lower limit becomes more negative by 2.33 eV, the difference between the ionization energies of C and H.

A total of 22 velocity vector maps were determined. We show here a minimum set of results which illustrate the major features of the reaction dynamics.

The maps in Figs. 1-6 show the evolution of the product distribution for the reaction of $C^+$ with $H_2$ (or $D_2$) as the initial relative energy is increased from 2.86 eV to 7.1 eV. The distribution of $CH^+$ at the lowest relative energy displayed here (Fig. 1) shows a high degree of symmetry about the $\pm$ 90° axis. However, there is a modest but easily discernable intensity maximum in the small angle region, close to the center of mass velocity. Another of our experiments performed at a relative energy of 2.0 eV shows a very similar distribution, with a slight forward peaking still evident.

Figure 2 shows that at an initial relative energy of 3.44 eV, the $CH^+$ distribution retains some symmetry about the $\pm$ 90° axis, but the forward peak is quite prominent. The intensity maximum falls at Q = -2.95, which corresponds to an internal excitation energy for $CH^+$ of 2.5 eV, approximately 60% of the minimum needed to dissociate $CH^+$ to $C^+$ and H. Rather little product is found near Q = -1.5 eV, which at this relative energy corresponds to spectator

stripping at 0° or to the elastic spectator model at other angles.

The distribution of $CD^+$ from the $C^+$-$D_2$ reaction at the same relative energy is shown in Fig. 3. The distribution is very similar to that found for $CH^+$ from $H_2$ at the same relative energy, except that the $CD^+$ appears to be if anything more highly excited internally than the $CH^+$. The slight asymmetry and modest forward peaking of the distribution are again evident.

These experiments performed at 3.44 and 3.6 eV are of particular interest since they can be compared to the experiment performed at the same energy by Iden, Liardon, and Koski[12] on the $C^+$-$D_2$ system. The map reported by these workers shows the $CD^+$ distribution peaked at the center-of-mass velocity, and quite symmetric about the $\pm$ 90° axis. On the other hand, Koski et al also report the value of Q for the intensity maximum at several other initial relative energies, and in every case, these most probable Q values are more positive than the Q corresponding to a peak at the center-of-mass velocity. If the experimental peaks in fact lie in the small angle region, most of the results of Koski et al[12] may be more consistent with our findings than a comparison of the maps at 3.4 eV would suggest.

It is worthwhile at this point to comment on the unfortunate tendency in the ion-molecule literature to use the terms "collision complex distribution" and "a distribution

peaked at the center-of-mass" as synonymous phrases. In the first place, there is no reason why direct interactions can not give product velocity vector distributions peaked at the centroid velocity, and such phenomena have been observed.[14,15,18] Second, the fact that the density of final translational states is an increasing function of the final relative velocity with a zero at centroid shows that the centroid velocity will very likely be at least a local minimum in the true intensity distribution even when there is no potential energy barrier in the exit channel surface. The calculated density of final states often rises rather rapidly as the final relative energy increases from zero, and hence the distribution may reach a maximum at a velocity quite close that of centroid. Detection of such a distribution with an instrument of relatively low resolution may give the impression of a peak at centroid, when in fact a sharp minimum exists. To avoid confusion and ambiguity, the phrases "peaked at centroid" and "collision complex mechanism" should not be used to imply one another.

Figure 4 shows the $CH^+$ distribution obtained from collisions of $C^+$ with $H_2$ at 5.03 eV relative energy. The intensity peak in the small angle region is now quite prominent, but product at this most probable velocity is still more internally excited (3.4 eV) than would correspond to spectator stripping (2.9 eV). The circle in Fig. 4 labeled $Q$ = -4.5 eV represents the limit of stability for the ground state of $CH^+$

and all excited states which dissociate to $C^+(^2P)$ and $H(^2S)$. Thus velocities which correspond to $Q < -4.5$ eV constitute a "forbidden" region for these low lying states of $CH^+$. The presence of $CH^+$ in this region may indicate that in some collisions $CH^+$ is formed in states which dissociate to C and $H^+$, or that some $CH^+$ is formed with internal energy greater than the dissociation energy, but is held together by a rotational barrier. However, it is likely that most of the intensity in the forbidden region of Fig. 4 is a consequence of the finite beam energy spread, detector resolution, and thermal motion of the target gas.

The asymmetry of the distribution about the $\pm$ 90° axis makes it clear that the reaction mechanism at this energy is best described as a direct interaction. However, the substantial angular width of the forward peak, and the rather broad speed distribution at all angles suggests that during the collision, the system passes through regions of a potential surface where all three atoms are simultaneously strongly coupled. In particular, the forward scattered product, which one can assume comes principally from grazing collisions, does not reach a maximum intensity at the spectator stripping velocity. This shows that even in these collisions, the freed hydrogen atom interacts strongly enough with the incipient $CH^+$ to be accellerated and to carry off energy which in a spectator process would appear as internal excitation of $CH^+$.

The 5.03 eV experiment in Fig. 4 lies in energy between two product velocity maps reported by Iden, Liardon and Koski.[12] These two maps, done at relative energies of 4.4 and 5.98 eV, both show a slight forward-back asymmetry with some forward peaking developing at the higher energy. However, neither is as sharply peaked as the map we show in Fig. 4.

The distribution of $CH^+$ from $C^+$-$H_2$ collisions at an initial relative energy of 7.06 eV is shown in Fig. 5. The forward peak is now fully developed, with the maximum intensity falling very close to the spectator stripping velocity. An intensity minimum or crater appears in the forbidden region inside the Q = -4.5 eV circle. There is scattering of low, but easily detectable, intensity in the large angle regions near 180°. Thus the general appearance of the map in Fig. 5 is quite consistent with formation of $CH^+$ by a direct interaction process.

The low intensity ridge which occurs in the large angle region of Fig. 5 does not appear in the maps of the $CD^+$ distributions determined at the same and higher relative energies by Iden, Liardon, and Koski.[12] We believe that this discrepancy is related to their use of a retarding potential analyzer to obtain a product energy distribution at various angles. With this method, detecting a low intensity peak at low velocity in the presence of a high intensity peak at greater velocity is rather difficult, since it requires

the very precise measurement of small changes in a relatively large signal. In contrast, a deflection analyzer such as the 90° electrostatic energy analyzer in our apparatus passes only a narrow band of energies at any time, and the measurement of a small intensity peak in the presence of a component of much higher intensity and velocity does not present a problem. It is this feature that has allowed us to measure for many systems,[7,18,22] the distribution of non-reactively scattered ions at the large center-of-mass angles which coincide in the laboratory with the direction of the primary projectile ion beam. This has not yet been done and probably can not be done with a retarding potential energy analyzer.

Comparison of the distributions of the two isotopic products of the reaction of $C^+$ with HD can provide further elucidation of the reaction dynamics. Figure 6 shows the $CH^+$ distribution, and Fig. 7 the $CD^+$ distribution from reaction of $C^+$ with HD at 3.5 eV relative energy. The two distributions resemble each other closely. The relative intensities are also qualitatively consistent with the isotope effect measured by Henchman *et al*[13] for the $C^+$-HD reaction. Figures 6 and 7 are also very similar to the maps in Fig. 2 and 3, where the products of the reaction of $C^+$ with $H_2$ and $D_2$ are shown.

The great similarity of the product distributions from the three isotopic targets is in marked contrast with

findings from this laboratory[7,17,23] concerning isotope effects for reactions which proceed by a direct interaction mechanism. That is, for the direct reactions of $N_2^+$, $O^+$, and, at high relative energy, $O_2^+$ with HD, the angular distribution of the two isotopic products show very significant and sometimes rather spectacular differences. The great similarity of the isotopic product velocity vector distributions from the reaction of $C^+$ with $H_2$, $D_2$ and HD therefore reinforces the idea that these processes are dominated at low relative energies by a mechanism which involves strong coupling between all three atoms.

Figures 8 and 9 show, respectively, the distribution of $CH^+$ and $CD^+$ from $C^+$-HD collisions at 4.91 eV relative energy. While superficially similar, the two distributions show significant differences. In particular, the $CH^+$ distribution is the more asymmetric, with a forward to back intensity ratio at a given value of Q clearly greater than the same ratio in the $CD^+$ distribution. This greater propensity for the hydrogen isotope to appear in the forward scattering region is evidently characteristic of direct interaction processes, since it has been observed[7,17,23] in the reactions of $N_2^+$, $O^+$, and $O_2^+$ with HD.

This conclusion is strengthened by comparison of Figs. 10 and 11, which show the $CH^+$ and $CD^+$ distributions obtained at relative energies of approximately 7.14 eV. The $CH^+$ distribution remains clearly forward peaked, but

in the $CD^+$ distribution, the forward and backward regions have quite comparable intensities. The propensity for the deuterium carrying product to move to larger scattering angles as the collision energy is increased has also been observed previously[7,17,23] in direct interaction processes. Thus the isotopic distributions leave little doubt that the reaction of $C^+$ with hydrogen proceeds by a direct interaction mechanism at relative energies above 5 eV.

It should be noted that in Fig. 11. the spectator stripping velocity lies in the "forbidden" velocity region where $CD^+$ in its electronic ground state is unstable to dissociation to $C^+$ and D. It is probably for this reason that the $CD^+$ intensity in the small angle region of Fig. 11 is considerably smaller than the corresponding $CH^+$ intensity shown in Fig. 10. In the later case, the spectator stripping velocity lies in a region which the product in its ground state is stable to dissociation.

In both Figs. 10 and 11, there is noticeable intensity in the forbidden region inside the Q = - 4.5 eV circle. This again raises the question of whether some collisions form $CD^+$ in states which dissociate to C and $H^+$. Such states would be stable for Q values as low as -6.8 eV. The possibility that this does occur seems somewhat strengthened by the fact that in the experiment of Iden, Liardon and Koski[12] performed at 8.48 eV relative energy, the product peak lies at a Q value of approximately -7 eV.

Figures 12-14 show the evolution of the distribution of the $C^+$ scattered non-reactively from $H_2$. These distributions have a number of significant features in common. At angles of 90° and smaller, there is a well defined ridge of intensity which lies on or quite close to the circle labeled Q = 0, the locus of elastic scattering. The intensity of this elastic component diminishes as the angle increases in the manner expected for a feature arising from a direct or quasi-impulsive scattering process. At angles quite near 180°, the intensity of this elastic component is considerably attenuated. Evidently, the nearly head-on collisions which could produce elastic scattering in this very large angle region in fact lead to reaction or very inelastic scattering. It is of interest that only the very large angle-small impact parameter elastic scattering seems appreciably attenuated. This is consistent with the relatively small total reaction cross section ($\lesssim 2 \times 10^{-16}$ cm$^2$) determined by Koski and coworkers.[10]

The distributions in Figs. 12-14 all show substantial $C^+$ intensity in the regions close to the center-of-mass velocity. Extremely inelastic scattering of this type has been observed in the $O_2^+$-$H_2$ system,[18] where it is believed that at low relative energy most reactive and inelastic collisions involve a long-lived $H_2O_2^+$ intermediate. On the other hand, the non-reactive collisions between such systems as $Ne^+$-$H_2$, $Ar^+$-$D_2$, and $Na^+$-$D_2$, which do not involve long-lived intermediates, are much less inelastic. Thus we feel that the

non-reactive scattering in the $C^+$-$H_2$ system is a convincing piece of evidence that a strongly coupled collision intermediate occurs in this system.

A feature of the distribution in Fig. 14 requires comment. At the high relative energy of 7.05 eV the very inelastic scattering near the center-of-mass velocity remains prominent, but the inelastic component reaches a peak in the small angle region. This type of behavior has been observed[17,18] in the non-reactive scattering of $N_2^+$ and $O_2^+$ from $H_2$ and $D_2$. The inelastic maximum in Fig. 14 lies near the small cross which marks the velocity that $CH^+$ would have if it were formed by the spectator stripping process. This raises the question of whether the inelastically scattered $C^+$ in this region comes from the dissociation of $CH^+$ which had been formed by the spectator stripping process. However, at a relative energy of 7.1 eV, $CH^+$ formed by spectator stripping has an internal energy of 3.7 eV, which is less than the 4.1 eV necessary to dissociate $CH^+$ to $C^+$ and H. Moreover, in view of the rather strong coupling between all atoms which apparently exists in this system, it seems likely that the major contribution to the inelastic peak in Fig. 14 comes from processes which are more complicated than stripping followed by dissociation.

The experimental evidence presented here makes it clear that at low relative energies the $C^+$-$H_2$ reaction proceeds by a mechanism which is quite different from the

direct interaction process which is operative in exoergic hydrogen atom transfer reactions.[15,24] While the substantial symmetry of the $CH^+$ distributions seems to invite the conclusion that the reaction involves a long-lived $CH_2^+$ intermediate, this description is too simplified. In no case, even at the lowest relative energies, have we found the $CH^+$ or $CD^+$ distribution to be completely symmetric. A peak is always present in the small angle region.

There are two obvious interpretations of this slight asymmetry. The first alternative is that the $C^+$-$H_2$ collisions exemplify an "osculating" complex,[25] where a strong but transient interaction lasting approximately one rotation period occurs. Use of the RRKM theory of unimolecular reactions to calculate the lifetime of $CH_2^+$ with a total energy in the range encountered in these experiments gives values in the range $5 - 10 \times 10^{-14}$ sec, which coincides with the distributions of rotation periods that occur. While calculated lifetimes this small are of questionable accuracy, their qualitative nature is somewhat edifying. Since an average lifetime of several rotational periods is necessary[25] before a collision complex produces a truly symmetric distribution, the description of the $C^+$-$H_2$ reaction as involving an osculating complex seems appropriate.

The second possibility, which may not exclude the first, is that the appearance of a forward peak on an otherwise symmetric distribution is a manifestation of

reactive scattering from more than one potential surface. Indeed, $C^+(^2P)$ approaching $H_2(^1\Sigma)$ collinearly produces both $^2\Sigma$ and degenerate $^2\Pi$ surfaces. These become $^2A_1$, $^2B_1$, and $^2B_2$ for approach of the $C^+$ along the perpendicular bisector of $H_2$. To decide which of these surfaces may have characteristics that can produce the observed scattering we will investigate the electronic state correlation diagram for this system.

Figure 15 is a partial correlation diagram for some of the lower electronic states of the $C^+$-$H_2$ system. While the energies of the reactant and product states as well as the ground state of the symmetric $CH_2^+$ intermediate are known[26,27] or have been calculated[28,29] the position of all other states has at best qualitative significance. On the left side of the diagram an approach of the $C^+$ (or C) along the perpendicular bisector of the $H_2$ (or $H_2^+$) bond is assumed, and consequently the states are labeled in terms of the symmetry species of the $C_{2v}$ point groups. On the far right of the diagram, $C^+$ is assumed to approach $H_2$ collinearly, and the intermediate separates to products in the same manner.

Starting with the collinear correlations, we see that as the ground state carbon ion $C^+(1s)^2(2s)^2(2p)^1\ ^2P_u$ approaches $H_2\ ^1\Sigma_g^+$, either the $^2\Sigma$ or the doubly degenerate $^2\Pi$ state of linear $CHH^+$ may be formed. The molecular orbital configuration of the $^2\Sigma$ state is analogous to the lowest configuration of $H_3$, in that both are three-center three-electron systems. That is,

in addition to the two non-bonding valence electrons on the carbon atom, there are two electrons in a totally bonding three-center orbital, and one electron in an orbital which is weakly antibonding between the end atoms, and largely non-bonding between adjacent atoms. On this $^2\Sigma$ surface, there may or may not be a potential energy barrier in excess of the reaction endoergicity, but it is very unlikely that there is a substantial potential minimum. The surface leads directly to the ground states of the products, $CH^+(^1\Sigma)$ and $H(^2S)$.

In the linear $^2\Pi$ states, there is one $2p\pi$ electron, a non-bonding electron pair centered on the carbon atom, and two electrons in the totally bonding three-center orbital. Since there are no antibonding electrons it is likely that the $^2\Pi$ surface lies below the $^2\Sigma$ surface at most internuclear distances. Indeed, calculations based on the Cashion-Herschbach[30] semi-empirical procedure for relating the energy of a three-atom system to the properties of its constituent diatomics show that the $^2\Pi$ state does lie below the $^2\Sigma$ state as the reactants approach each other. As the system separates to products, the $^2\Pi$ state starts to correlate with $CH(^2\Pi)$ and $H^+$. However, an avoided crossing occurs[31] which makes the lowest $^2\Pi$ surface separate to $CH^+(^3\Pi)$ and $H(^2S)$.

We consider now the approach of $C^+(^2P_u)$ along the perpendicular bisector of the $H_2$ bond. Of the three states $^2B_2$, $^2B_1$, and $^2A_1$ which can be formed, none has the valence orbital configuration of the ground state of symmetric $CH_2^+$, $(2a_1)^2(1b_2)^2(3a_1)^1\ ^1A_1$, or of the very low lying excited state

$(2a_1)^2(1b_2)^2(1b_1)^1\,{}^1B_1$. In fact, the $^2A_1$ state formed from the reactants has the configuration $(2a_1)^2(3a_1)^2(4a_1^*)^1$, in which the $4a_1^*$ antibonding orbital is occupied, and the $1b_2$ bonding orbital is empty. Consequently, the energy of this $^2A_1$ state probably increases as the reactants approach each other, and this surface may not lead to reaction in very low energy collisions. However, the initial $^2A_1$ surface does lead to ground state $CH_2^+$ through an avoided crossing with the $^2A_1$ state which originates with $C(^1D)$ and $H_2^+(^1\Sigma)$. Therefore, moderate to high energy collisions on the $^2A_1$ surface may lead the system to the potential well associated with symmetric $CH_2^+$.

The $^2B_1$ surface formed from $C^+$ and $H_2$ initially corresponds to the valence orbital configuration $(2a_1)^2(3a_1)^2(1b_1)^1$ in which the bonding $1b_2$ orbital is again empty, but no antibonding electrons are present. Thus the $^2B_1$ surface may be rather flat until it encounters a second $^2B_1$ surface which originates with $C(^3P_g)$ and $H_2^+(^2\Sigma_u^+)$ and correlates to the lowest excited state of $CH_2^+$. The crossing of the adiabatic $^2B_1$ states is avoided, and consequently $C^+(^2P_u)$ and $H_2(^1\Sigma_g^+)$ can proceed adiabatically on the $^2B_1$ surface to a very low lying level of $CH_2^+$.

The $^2B_2$ state formed from $C^+(^2P_u)$ and $H_2(^2\Sigma_g^+)$ has the valence orbital configuration $(2a_1)^2(1b_2)^1(3a_1)^2$, and in strict $C_{2v}$ symmetry, leads to an excited state of $CH_2^+$. However, this $^2B_2$ surface crosses the $^2A_1$ surface which

leads to the ground state of $CH_2^+$. While this crossing is allowed in $C_{2v}$ symmetry, it does not occur when the molecule is distorted, since both $^2A_1$ and $^2B_2$ become $^2A'$ states in $C_s$ symmetry. Thus we have an example of a conical intersection of surfaces.[32,33] If during the collision the system departs from $C_{2v}$ symmetry, as it frequently will, the ground state of $CH_2^+$ can be reached adiabatically. The correlation diagram shows these $CH_2^+$ ions in the $^2A_1$ state can dissociate to the ground state products $CH^+(^1\Sigma)$ and $H(^2S)$. Similarly, ions in the $^2B_1$ state dissociate to the first excited product state, $CH^+(^3\Pi)$ and $H(^2S)$.

It is of interest to relate the linear $CHH^+$ surfaces to those of the non-linear symmetric molecule. This can be done by examining the behavior of the 2s and the three 2p orbitals of carbon as linear $CHH^+$ is bent into $CH_2^+$ in the $C_{2v}$ conformation. The 2s orbital of linear $CHH^+$ evolves into the $2a_1$ bonding orbital of symmetric $CH_2^+$. The $\pi$p orbital perpendicular to the plane in which the molecule bends retains into $\pi$-character, and evolves as $\pi \rightarrow a'' \rightarrow 1b_1$. In contrast, the $2p\sigma$ and in-plane $2p\pi$ are mixed upon bending, and both become $a'$ orbitals which at certain conformations are degenerate. These orbitals eventually separate and become the $1b_2$ and $3a_1$ orbitals of symmetric $CH_2^+$. Because of the mixing of these orbitals in $C_s$ symmetry, the lowest energy configuration of linear CHH can evolve to the lowest energy configuration of $CH_2^+$. Thus when $CHH^+$ $(2s\sigma)^2(2p\sigma)^2(\pi)^1\ ^2\Pi$ is bent, one component

can form $CH_2^+(2a_1)^2(1b_2)^2(3a_1)^1\ ^2A_1$ and the other $CH_2^+(2a_1)^2(1b_2)^2(1b_1)^1\ ^2B_1$, which are the ground and first excited states of the molecule. Since linear $CHH^+(^2\Pi)$ very probably has a higher energy than bent symmetric $CH_2^+$ in either the $^2A_1$ or $^2B_1$ states, we can expect that collinear or nearly collinear collisions on the $^2\Pi$ surface will follow trajectories that lead them through or near the bent symmetric conformations. Thus, there is nothing to prevent these systems from fully exploring the rather deep potential well associated with $CH_2^+$.

The behavior of linear $CHH^+$ in the $^2\Sigma$ state may be rather different. In this case, all electrons are in $\sigma$ orbitals, the lowest two of which are the $2s\sigma$ bonding and $2p\sigma$ non-bonding orbitals. The highest $\sigma$ orbital at large $C^+$-$H_2$ distances is made up of an out-of-phase combination of the carbon $2p\sigma$ orbital and the hydrogen $\sigma_g$ orbital, and has one intranuclear nodal surface. As the molecule is bent, this orbital evolves to the $4a_1^*$ antibonding orbital of $CH_2^+$. Thus from linear $CHH^+(^2\Sigma)$ we approach $CH_2^+(2a_1)^2(1b_2)^2(4a_1^*)^1\ ^2A_1$, the highest of the three states which are formed when $C^+$ approaches $H_2$ broadside. It appears, then, that the $^2\Sigma$ surface has a minimum energy when $CHH^+$ is linear. However, it is worth noting again that the $^2A_1$-$^2A'$ state which is associated with linear $CHH^+(^2\Sigma)$ actually has an avoided intersection with the $^2A_1$ ground state of symmetric $CH_2^+$, as can be seen on the far left of Fig. 15. Thus, it seems possible that large distortions

of the $^2\Sigma$ state can lead adiabatically to the $^2A_1$ ground state of $CH_2^+$.

The conclusion that the ground state potential energy well is accessible to the reactants is contrary to that reached by Mahan[6] on the basis of molecular orbital correlations for the linear and symmetric bent conformations only. The state correlations employed here show that since the orbital configurations need not be conserved[34] as the reactants approach, the ground and lowest excited states of the intermediate are accessible. The difference in the conclusions reached using orbital and electronic state correlations shows the importance of using the latter whenever possible.

The most obvious interpretation of the correlation diagram is that in most collisions on the $^2\Pi$-$^2A_1$-$^2B_1$ surfaces, $C^+$ and $H_2$ pass through regions in which very strong interactions between all three particles occur. The time spent in or near this potential energy well may approach a rotational period. These conclusions are consistent with the appearance of the reactive scattering distributions, and the very inelastic features of the non-reactive scattering. The fact that nearly collinear collisions on the $^2\Sigma$ surface should lead to reaction by a direct or short-lived interaction might be responsible for the persistent slight asymmetry of the low energy reactive scattering. However, it is hard to understand how the contribution from nearly collinear collisions could appear <u>exclusively</u> as a feature in the small angle region. Perhaps even more significant is the fact that the small angle peak is

very close to the centroid velocity. This indicates a high degree of product internal excitation, greatly in excess of what has been observed for direct hydrogen atom transfer processes. It seems more likely that the forward peak is a consequence of the near equivalence of the rotational period and interaction lifetime of the collision complex. As indicated above, the state correlation diagram indicates that even systems on the $^2\Sigma$ surface may be able to reach the potential energy well of $CH_2^+$, and if this were the case, there would be little or no indication of reaction by direct interaction at low energy.

## Summary

The product velocity vector distributions from $C^+(H_2,H)CH^+$ and its isotopic variants show substantial but not perfect symmetry about the $\pm$ 90° axis of the barycentric system when the initial relative energy is in the 2-3 eV range. The non-reactive scattering at this energy shows a very inelastic component. This behavior is consistent with a strong interaction between all three atoms which lasts for approximately one rotational period of the $C^+$-$H_2$ collision complex. The electronic state correlation diagram shows that the relatively deep (4 eV) potential energy well of the ground state of symmetric $CH_2^+$ is accessible to the reactants, and can dissociate to the products $CH^+$ and H.. At relative energies above 3 eV, the reaction proceeds by a mechanism which becomes

increasingly direct or impulsive as the energy is increased. Even in this higher range of energies, however the breadth of the angular distributions and the deviations from spectator stripping attest to the strength of the three body interaction in this system.

Acknowledgement: This work was supported by the U. S. Atomic Energy Commission.

## References


1. Y. T. Lee, R. J. Gordon, and D. R. Herschbach, J. Chem. Phys. 54, 2410 (1971).
2. J. D. McDonald, P. R. LeBreton, Y. T. Lee, and D. R. Herschbach, J. Chem. Phys. 56, 769 (1972).
3. J. C. Tully, Z. Herman, and R. Wolfgang. J. Chem. Phys. 54, 1730 (1971).
4. M. G. Holliday, J. T. Muckerman, and L. Friedman, J. Chem. Phys. 54, 1058 (1971).
5. R. J. Donovan and D. Husain, Chem. Rev. 70, 489 (1970).
6. B. H. Mahan, J. Chem. Phys. 55, 1436 (1971).
7. K. T. Gillen, B. H. Mahan, and J. S. Winn, J. Chem. Phys. 58, 5373 (1973).
8. R. K. Preston and J. C. Tully, J. Chem. Phys. 54, 4297 (1971).
9. W. B. Maier, J. Chem. Phys. 46, 4991 (1967).
10. E. Lindeman, L. E. Frees, R. W. Rozett, and W. S. Koski, J. Chem. Phys. 56, 1003 (1972).
11. C. R. Iden, R. Liardon, and W. S. Koski, J. Chem. Phys. 54, 2757 (1971).
12. C. R. Iden, R. Liardon, and W. S. Koski, J. Chem. Phys. 56, 851 (1972).
13. P. F. Fennelly, M. J. Henchman, A. S. Werner and J. F. Paulson, (private communication).
14. G. Bosse, A. Ding. and A. Henglein. Z. Naturforschung A 26, 932 (1971).
15. A. Henglein, J. Phys. Chem. 76, 3883 (1972).

16. D. G. Truhlar, J. Chem. Phys. 51, 4617 (1969).

17. W. R. Gentry, E. A. Gislason, B. H. Mahan, and C. W. Tsao, J. Chem. Phys. 49, 3058 (1968).

18. M. H. Chiang, E. A. Gislason, B. H. Mahan, C. W. Tsao, and A. S. Werner, J. Phys. Chem. 75, 1426 (1971).

19. B. R. Turner, J. A. Rutherford, and D. M. J. Compton, J. Chem. Phys. 48, 1602 (1968).

20. J. L. Franklin et al., Natl. Std. Ref. Data Ser. Natl. Bur. Std., (U. S.) 26 (1969).

21. P. G. Wilkenson, Astrophys. J. 138, 778 (1963).

22. M. H. Cheng, M. H. Chiang, E. A. Gislason, B. H. Mahan, C. W. Tsao, and A. S. Werner, J. Chem. Phys. 52, 6150 (1970).

23. M. H. Chiang, B. H. Mahan, C. W. Tsao, and A. S. Werner, J. Chem. Phys. 53, 3752 (1970).

24. B. H. Mahan, Acc. Chem. Research, 1, 217 (1968).

25. G. A. Fisk, J. D. McDonald, and D. R. Herschbach, Disc. Faraday Soc. 44, 228 (1967).

26. G. Herzberg, Spectra of Diatomic Molecules (Van Nostrand, Princeton, N. J. 1950).

27. C. E. Moore, Natl. Bur. Std. (U. S.) Circ. No. 467 (1958).

28. S. Green, P. Bagus, B. Liu, A. McLean, and M. Yoshimine, Phys. Rev. A 5, 1614 (1972).

29. C. F. Bender and H. F. Schaefer, J. Mol. Spect. 37, 423 (1971).

30. J. K. Cashion and D. R. Herschbach, J. Chem. Phys. 40, 2358 (1964).

31. For a valuable review and references to earlier work on avoided crossings, see E. Nikitin in Chemische Elementarprozesse H. Hartmann, Ed. (Springer, Berlin 1968).

32. G. Herzberg, Electronic Spectra and Electronic Structure of Polyatomic Molecules (Van Nostrand, Princeton, N. J. 1968).

33. T. Carrington, Disc. Faraday Soc. 53, 27 (1972).

34. L. Cusachs, M. Krieger, and C. W. McCurdy, Int. J. Quantum Chem. S3, 67 (1969).

Figure Captions

Fig. 1. A contour map of the specific intensity in the center-of-mass system of $CH^+$ from collisions of $C^+$ with $H_2$ at 2.86 eV relative energy. Note the symmetry of most of the lower intensity contours about the $\pm$ 90° axis, and the slight peaking of intensity in the small angle region near the centroid velocity.

Fig. 2. A contour map of the specific intensity of $CH^+$ from collisions of $C^+$ with $H_2$ at 3.44 eV relative energy. Note the well-defined intensity peak in the small angle region falls at a much smaller speed than would correspond the spectator stripping, whose location is marked by a small cross.

Fig. 3. The distribution of the specific intensity of $CD^+$ from $C^+$-$D_2$ collisions at 3.64 eV relative energy. Note that the Q value at the small angle intensity maximum is nearly the same as in the corresponding $C^+$-$H_2$ experiment. (See Fig. 2.)

Fig. 4. The specific intensity of $CH^+$ from $C^+$-$H_2$ collisions at 5.03 eV relative energy. Note the well developed peak in the small angle region and the asymmetry about the $\pm$ 90° axis, which indicate reaction by a preponderantly direct interaction mechanism.

Fig. 5. The specific intensity of $CH^+$ from $C^+$-$H_2$ collisions at 7.06 eV initial relative energy. Note that for the first time, the small angle peak falls near the spectator stripping velocity which is marked by a small cross. For the first time, the intensity depression or crater in the small speed region is evident. The circle marked Q = -4.5 eV gives the smallest speed for which product is stable with respect to dissociation to $C^+$ and H.

Fig. 6. The specific intensity of $CH^+$ from the $C^+$-HD reaction at 3.52 eV. Note the considerable similarity to Figs. 2 and 3, which would be greater if the beam profiles were more nearly alike.

Fig. 7. The specific intensity of $CD^+$ from the $C^+$-HD reaction at 3.48 eV relative energy. Note the similarity to Fig. 2, 3, and 6.

Fig. 8. A contour map of the specific intensity of $CH^+$ from $C^+$-HD collisions at 4.91 eV initial relative energy. Although the asymmetry about the $\pm$ 90° axis indicates a direct interaction process, the intensity peak falls at much a smaller speed than expected for spectator stripping.

Fig. 9. A contour map of the specific intensity of $CD^+$ from $C^+$-HD collisions at 4.91 eV initial relative energy. Note that the $CD^+$ product is generally more excited internally than the corresponding $CH^+$ product shown in Fig. 8.

Fig. 10. A contour map of the specific intensity of $CH^+$ from $C^+$-HD collisions at 7.09 eV initial relative energy. Note that the intensity in the small angle region is much higher than at angles greater than 90°.

Fig. 11. A contour map of the specific intensity of $CD^+$ from $C^+$-HD collisions at 7.18 eV initial relative energy. Note that the spectator stripping velocity for $CD^+$ now lies in the forbidden zone where product is unstable with respect to $C^+$ and D. The nearly equal product intensity in the small and large angle regions is in sharp contrast to the behavior found in the $CH^+$ distribution in Fig. 10.

Fig. 12. The intensity distribution of $C^+$ scattered from $H_2$ at 2.87 eV initial relative energy. Notice the ridge of intensity at small angles which follows the Q = 0 (elastic) circle. Also, notice the high intensity near the centroid velocity, which corresponds to collisions in which the entire initial relative energy has been converted to the internal energy of $H_2$.

Fig. 13. The intensity distribution of $C^+$ scattered from $H_2$ at 3.51 eV initial relative energy. The elastic feature persists even at 150°, and the inelastic scattering near centroid is quite well defined.

Fig. 14. The intensity distribution of $C^+$ scattered from $H_2$ at 7.05 eV initial relative energy. The inelastic scattering is better defined, and appears to reach a maximum in the small angle region. The small cross marks the velocity which $C^+$ would have if it had come from the dissociation of $CH^+$ moving with the spectator stripping velocity.

Fig. 15. A correlation diagram for some of the electronic states of the $CH_2^+$ system. On the left side of the diagram, an approach of $C^+$ along the perpendicular bisect of the $H_2$ bond is assumed, while on the right side, $C^+$ approach $H_2$ collinearly. Only those states which are of direct or indirect importance in the chemical reaction are shown.

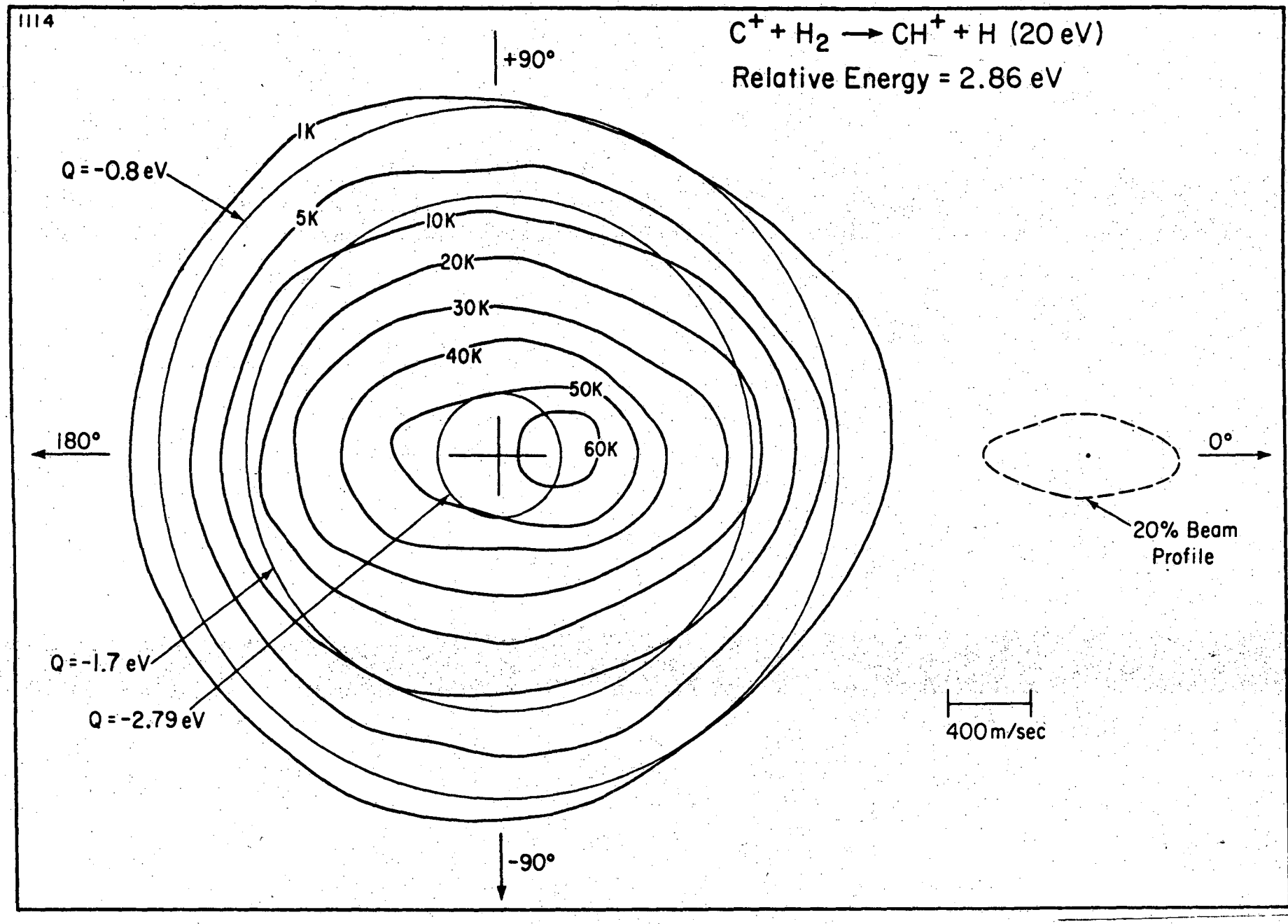


Fig. 1

XBL 739-1810

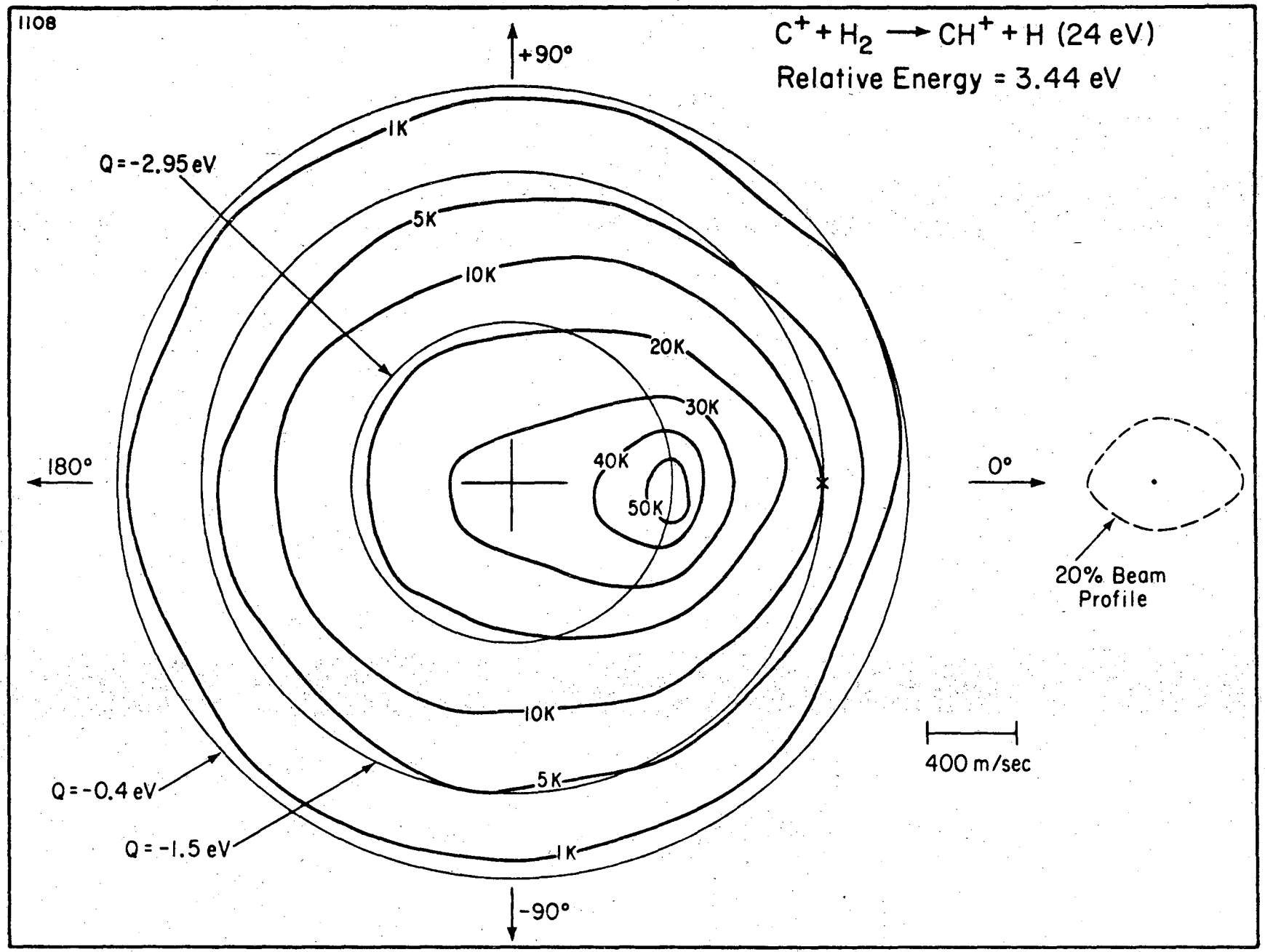


Fig. 2

XBL 739-1811

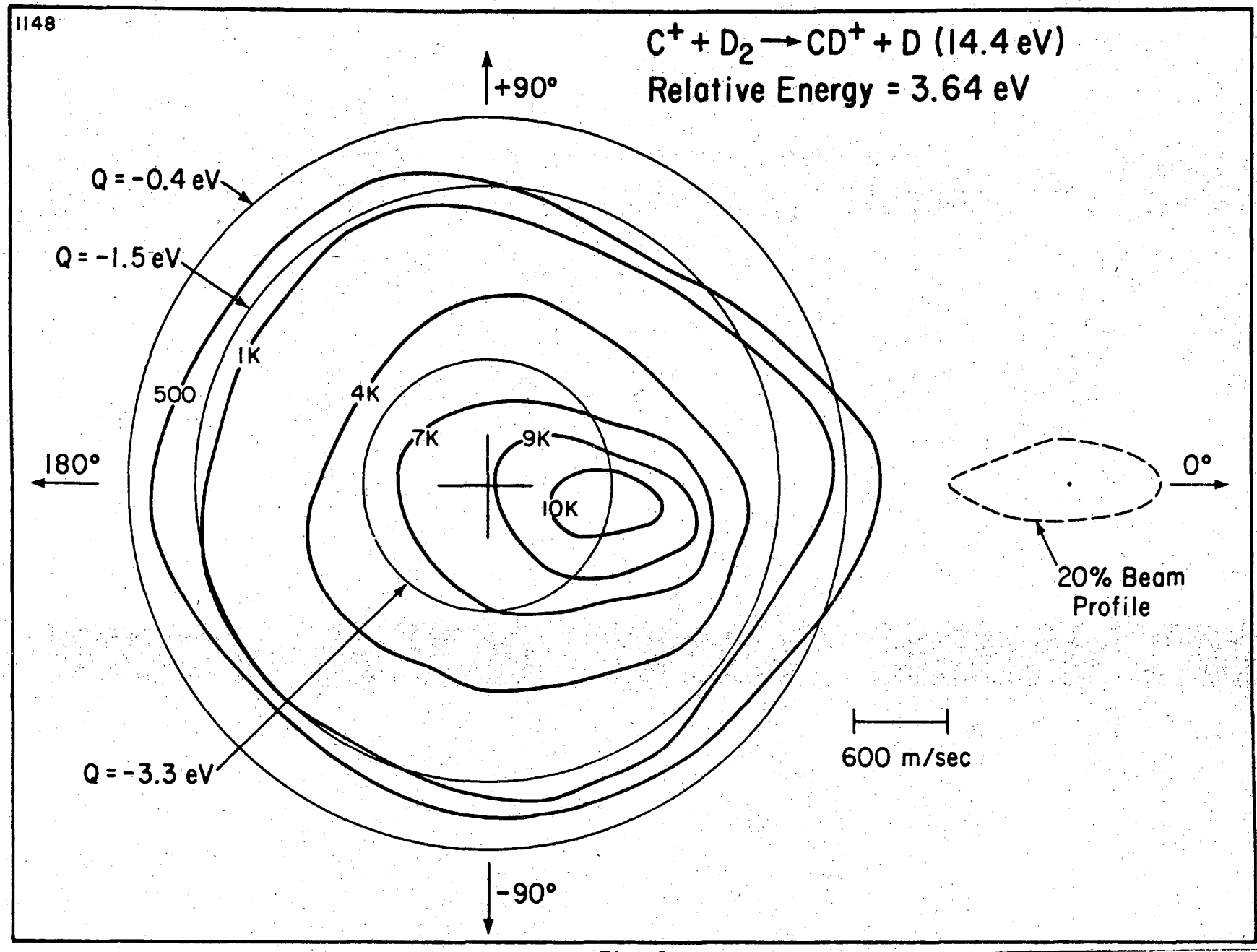


Fig. 3

XBL 739-1812

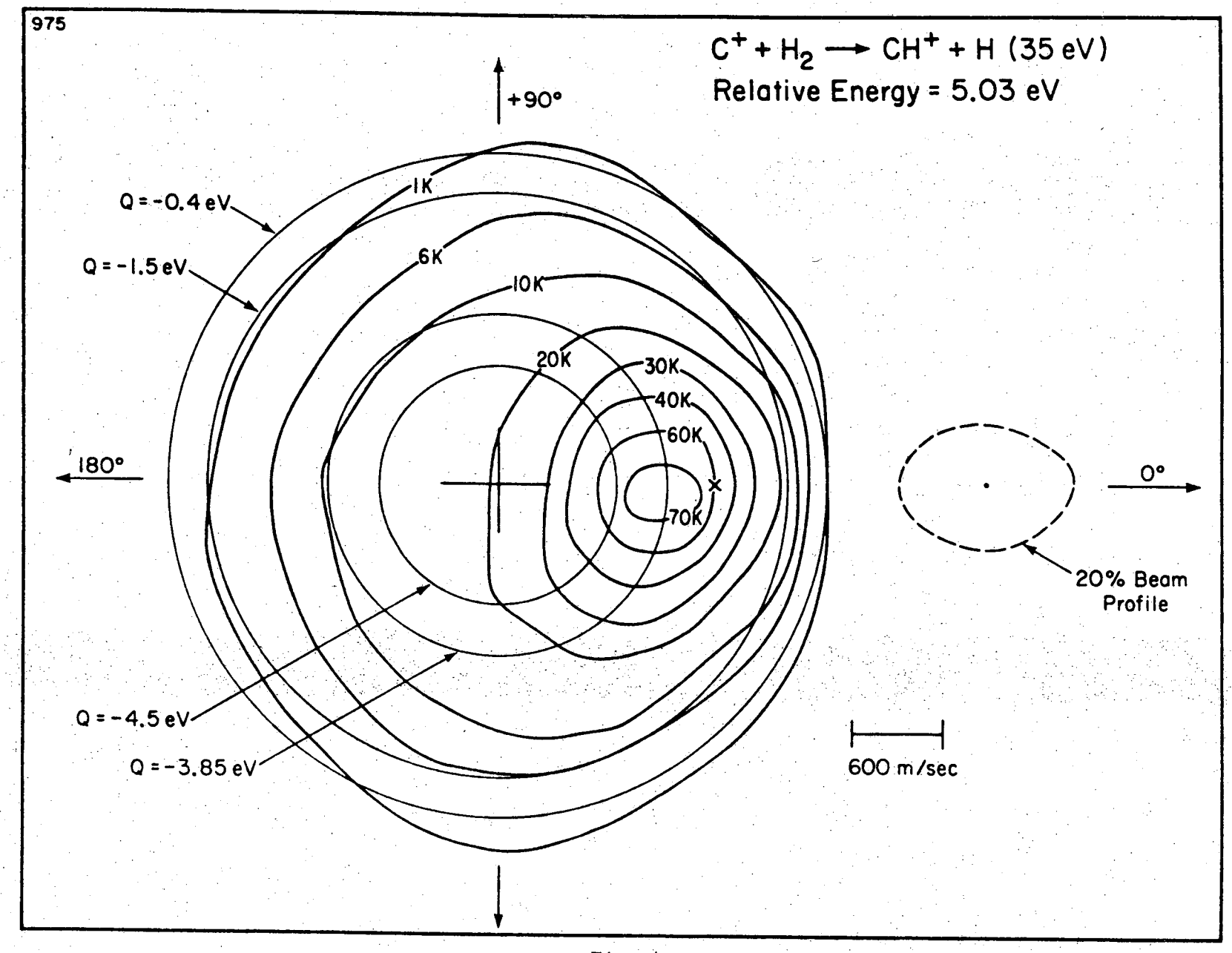


Fig. 4

XBL 739-1813

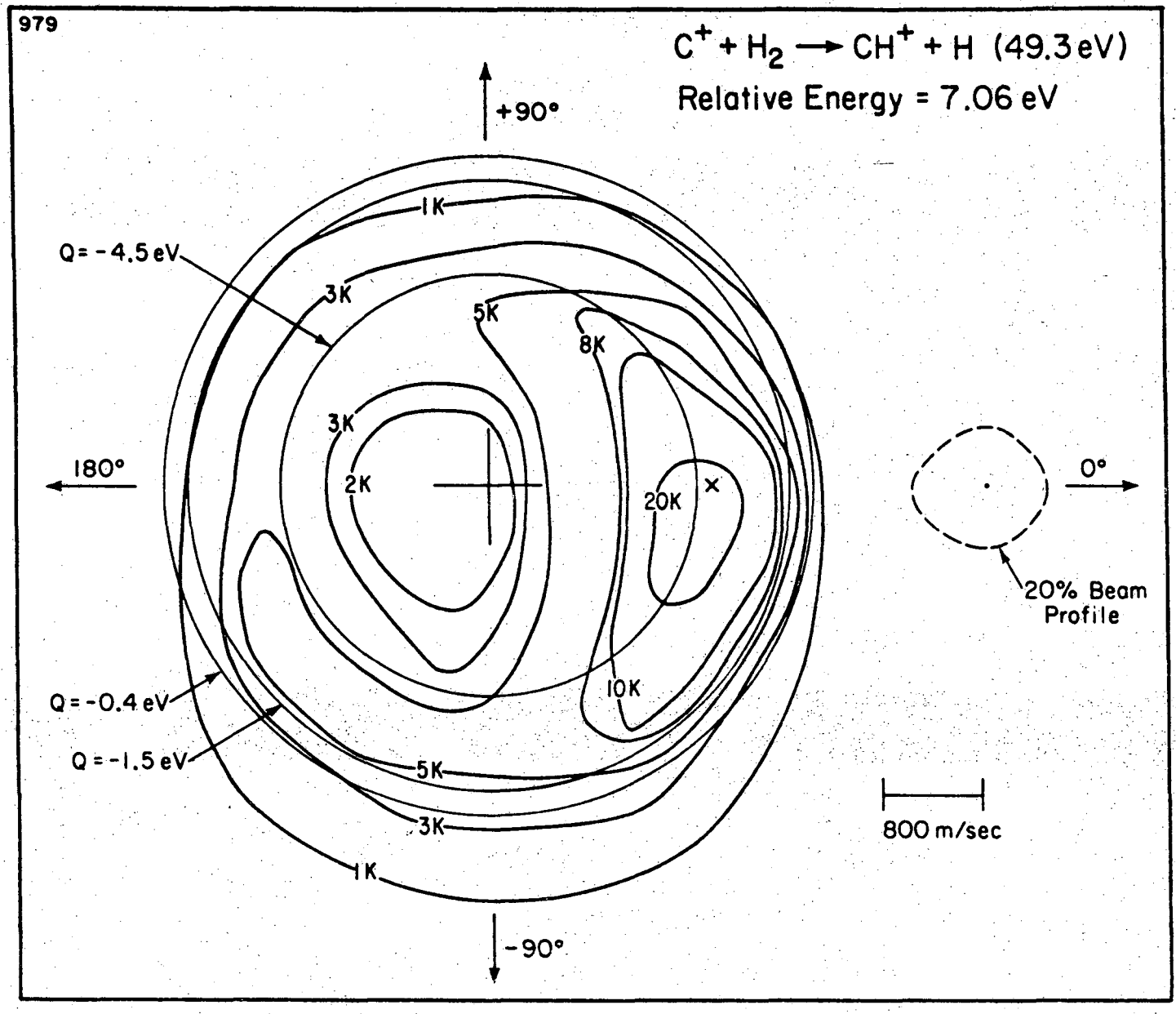


Fig. 5

XBL 739-1814

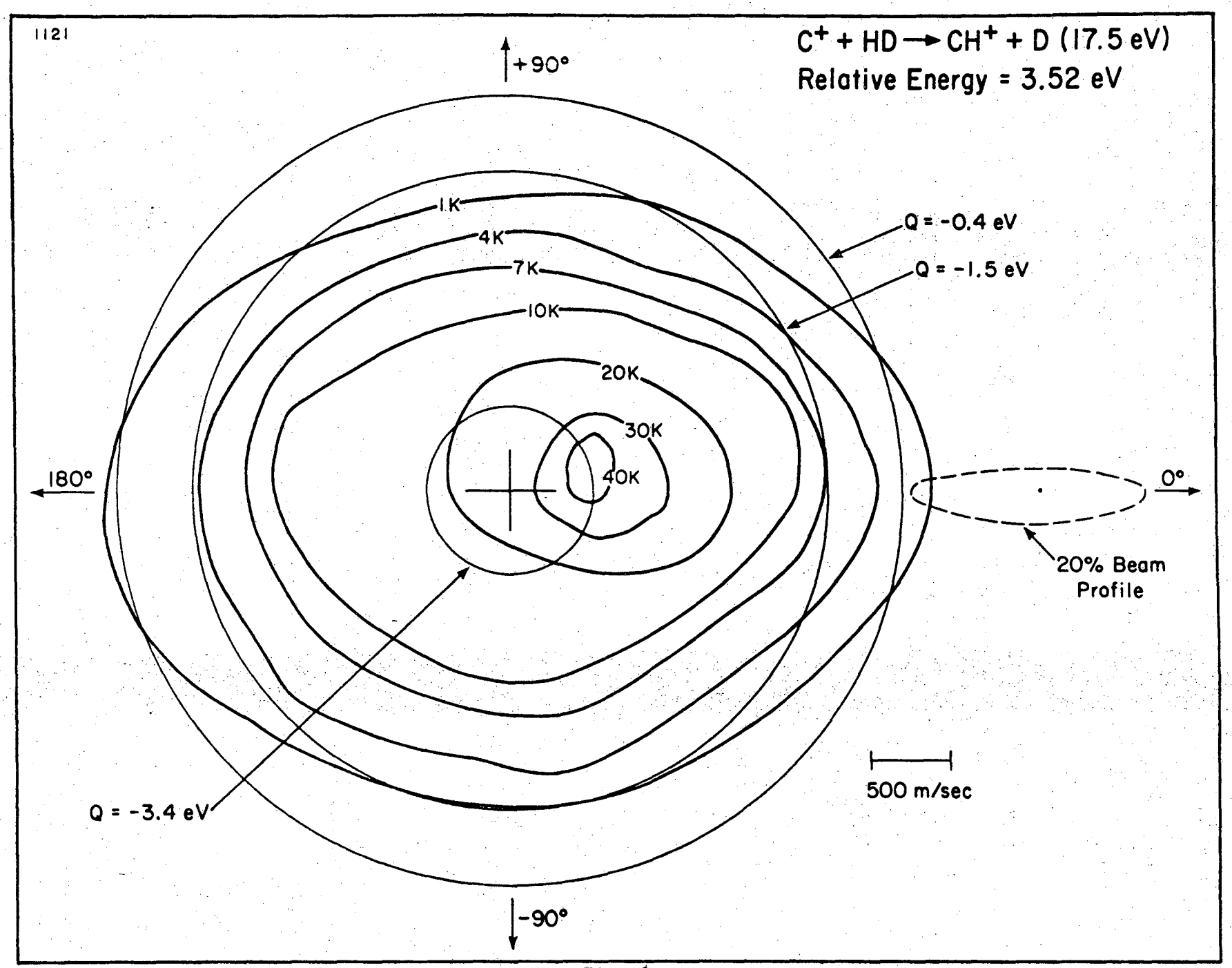


Fig. 6

XBL 739-1815

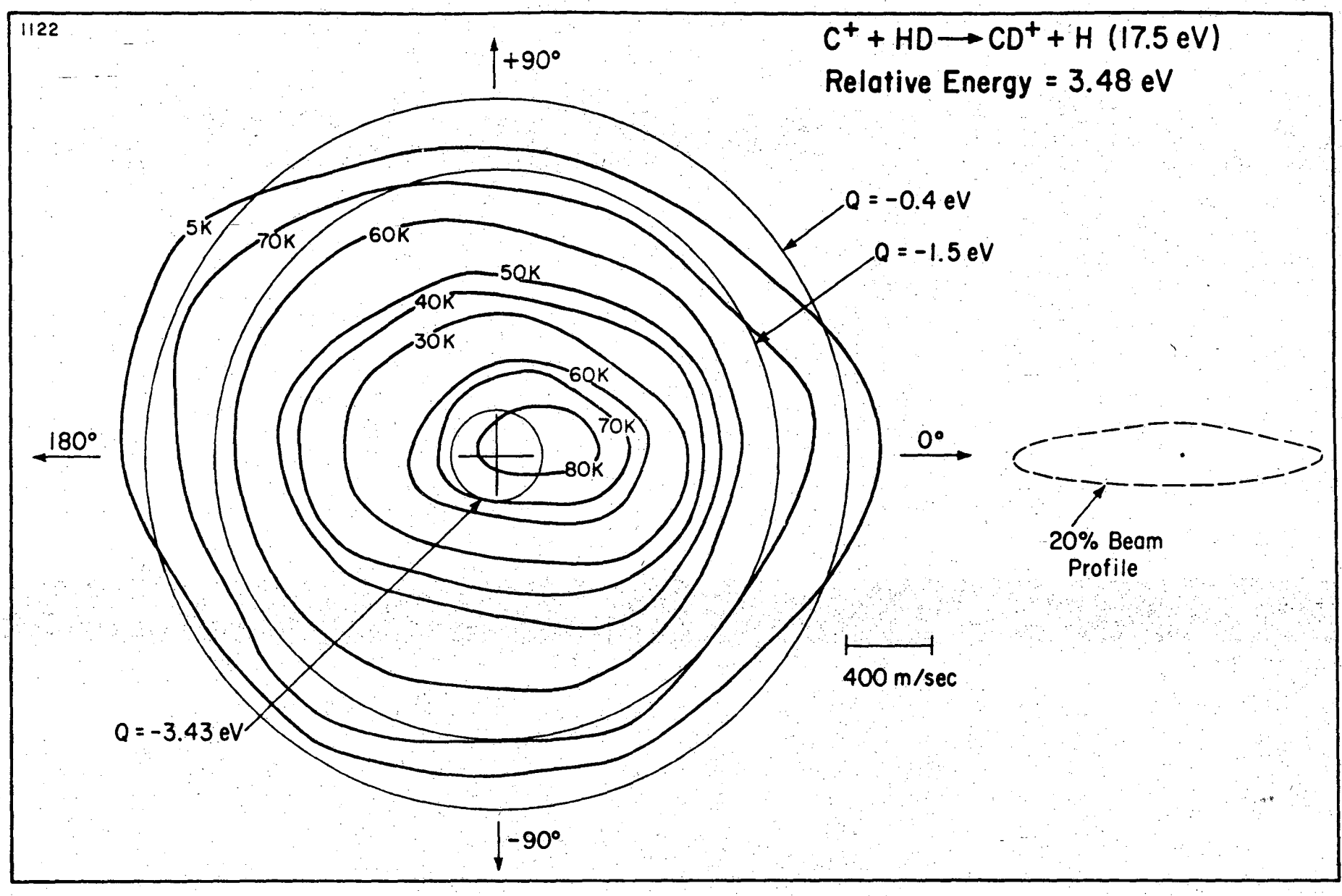


Fig. 7

XBL 739-1816

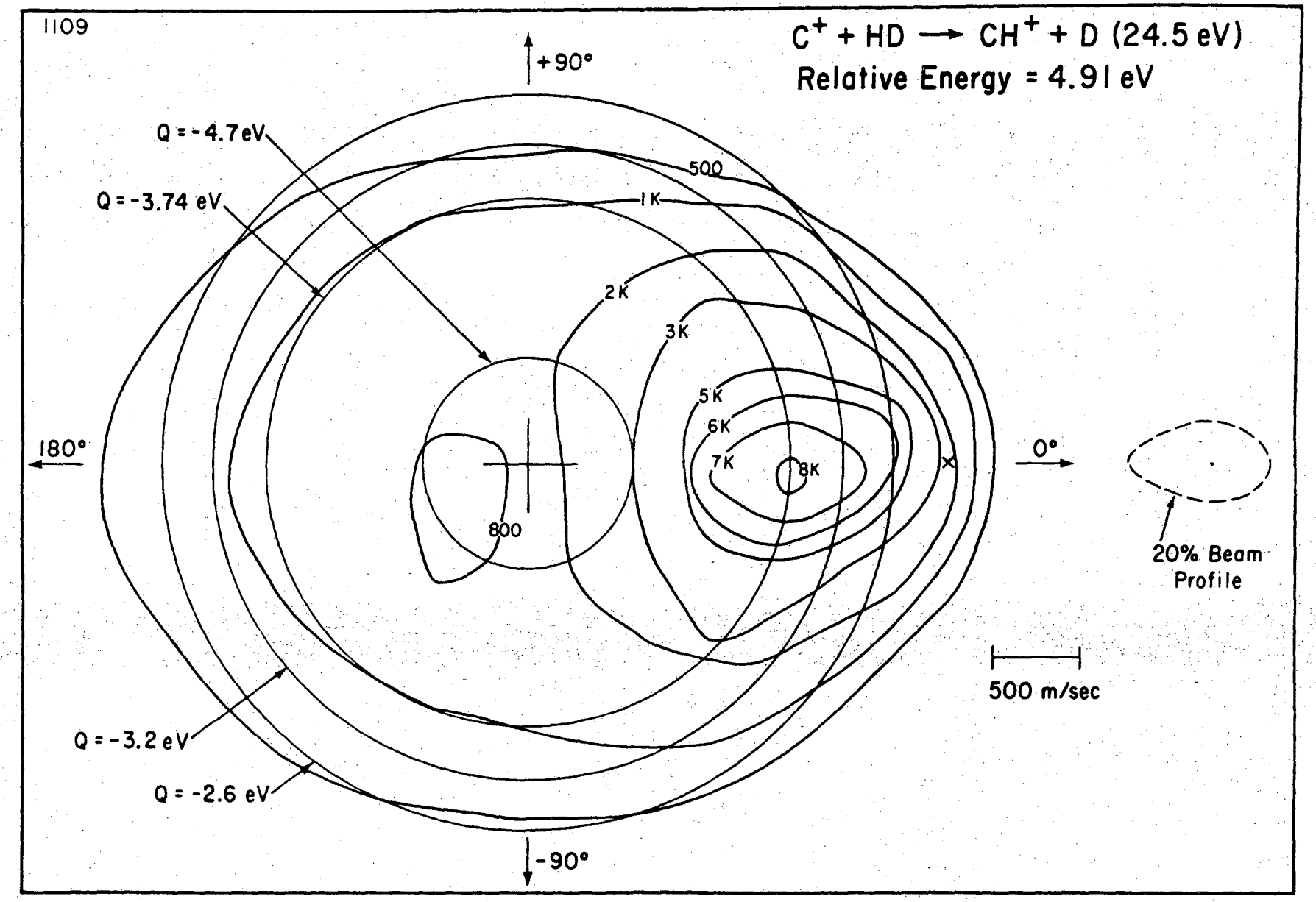


Fig. 8

XBL 739-1817

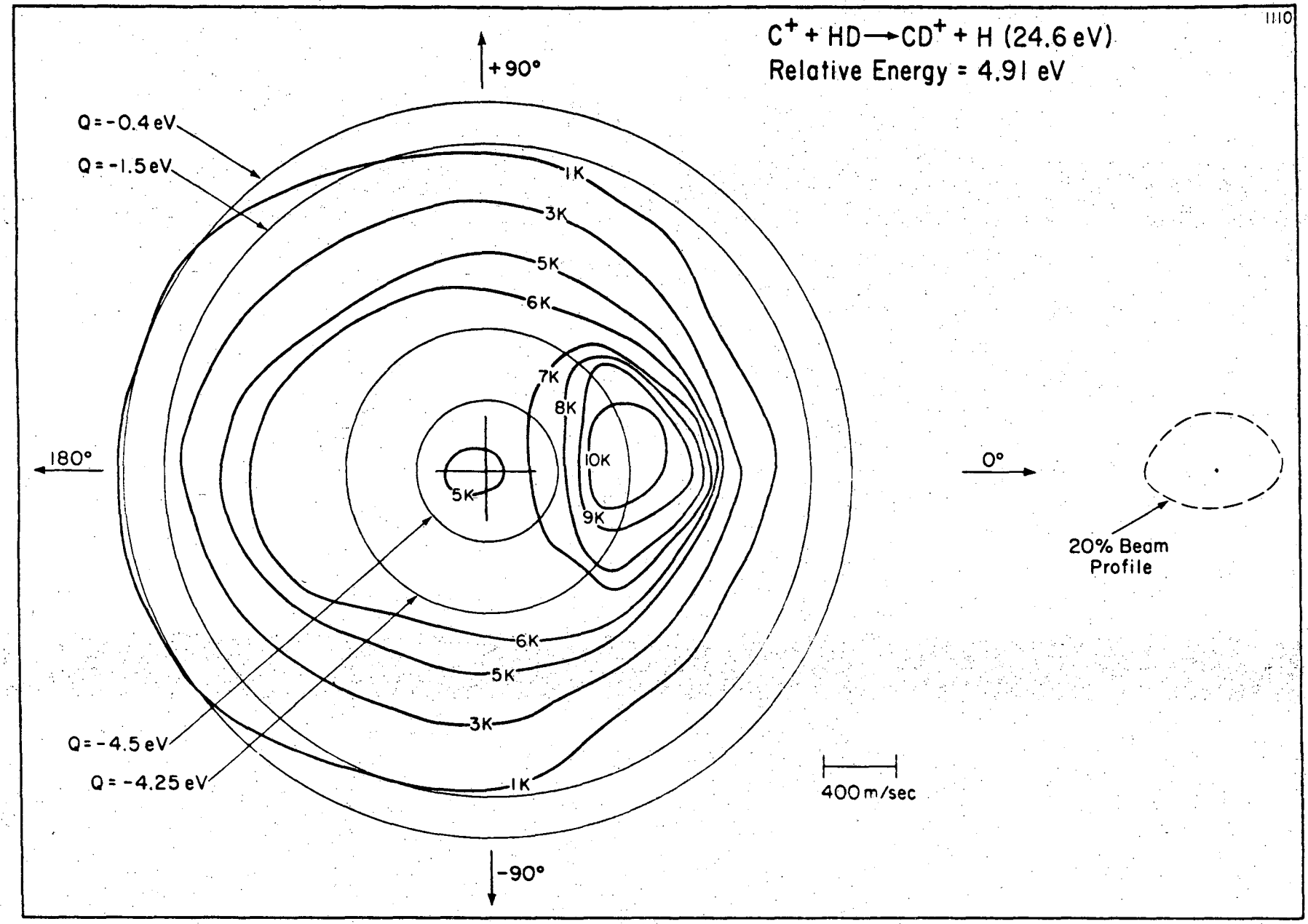


Fig. 9

XBL 739-1818

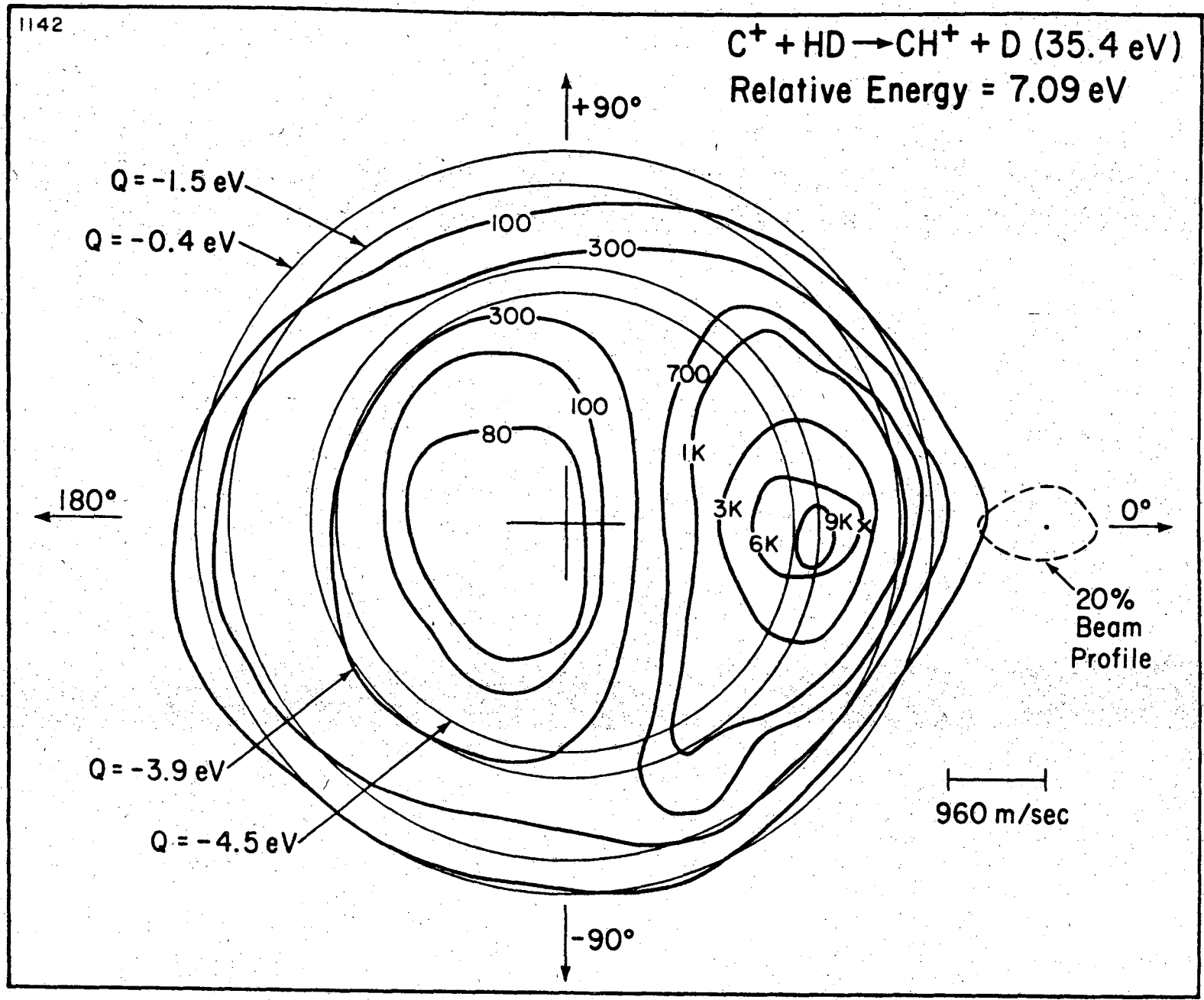


Fig. 10

XBL 739-1819

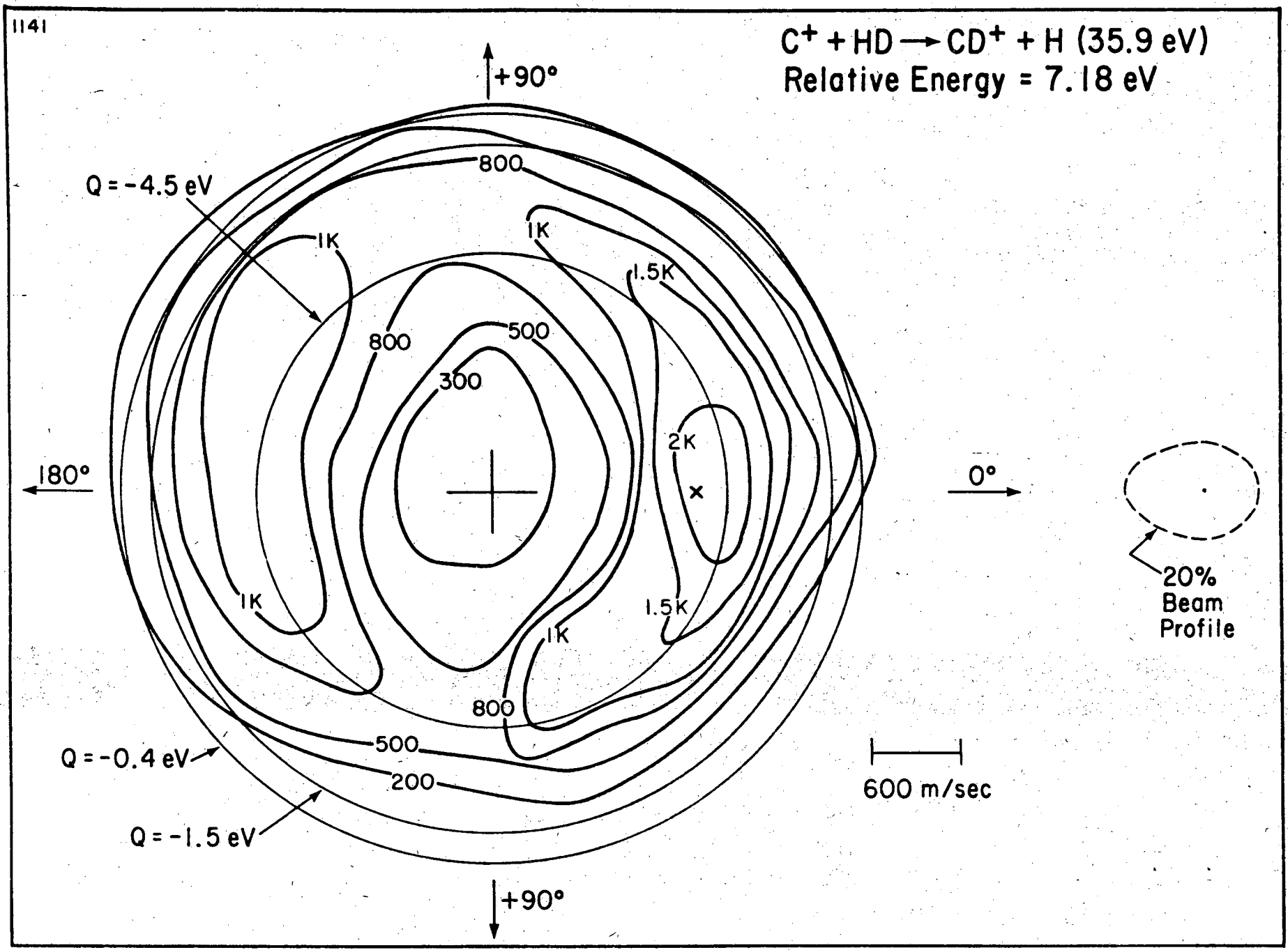


Fig. 11

XBL 739-1820

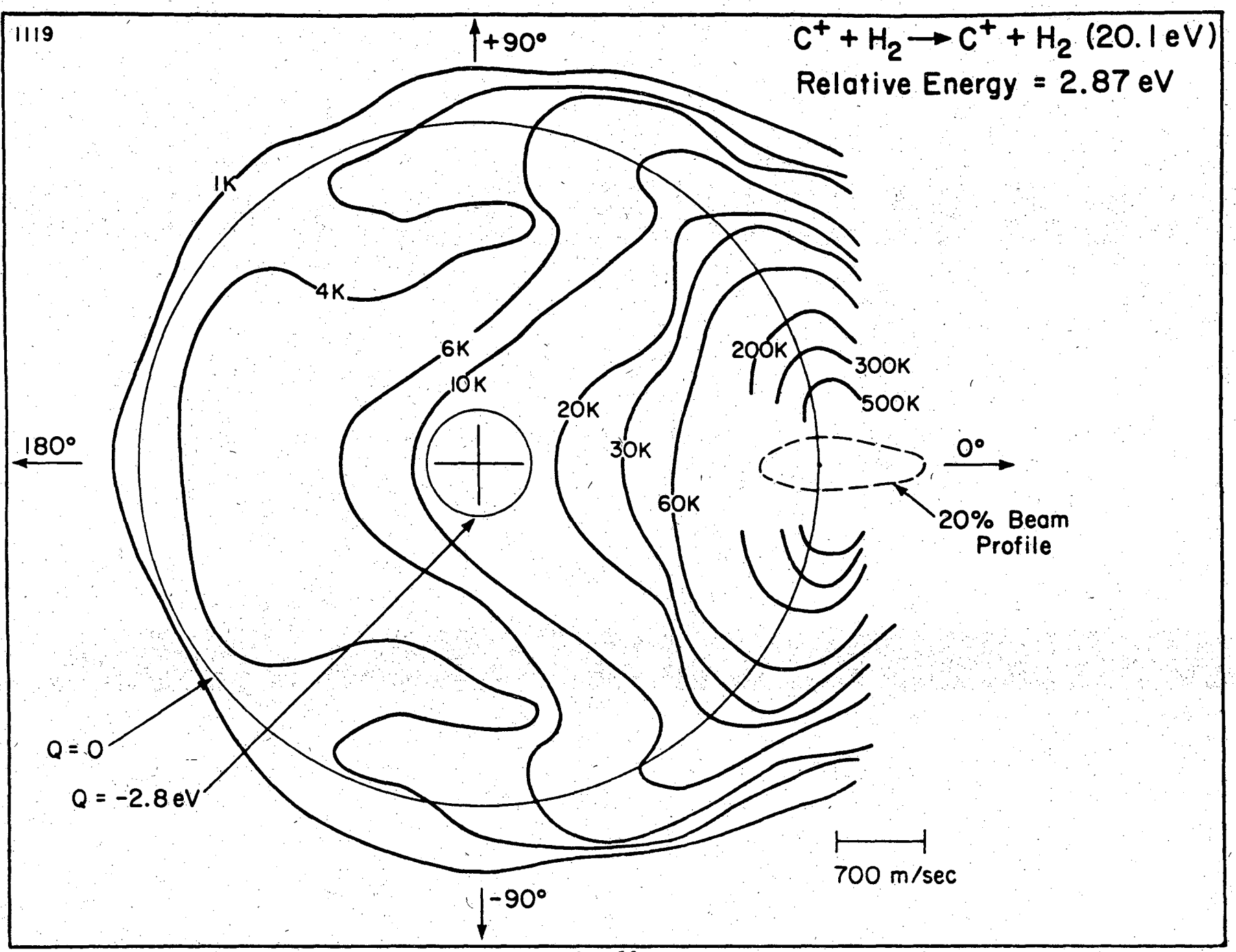


Fig. 12

XBL 739-1821

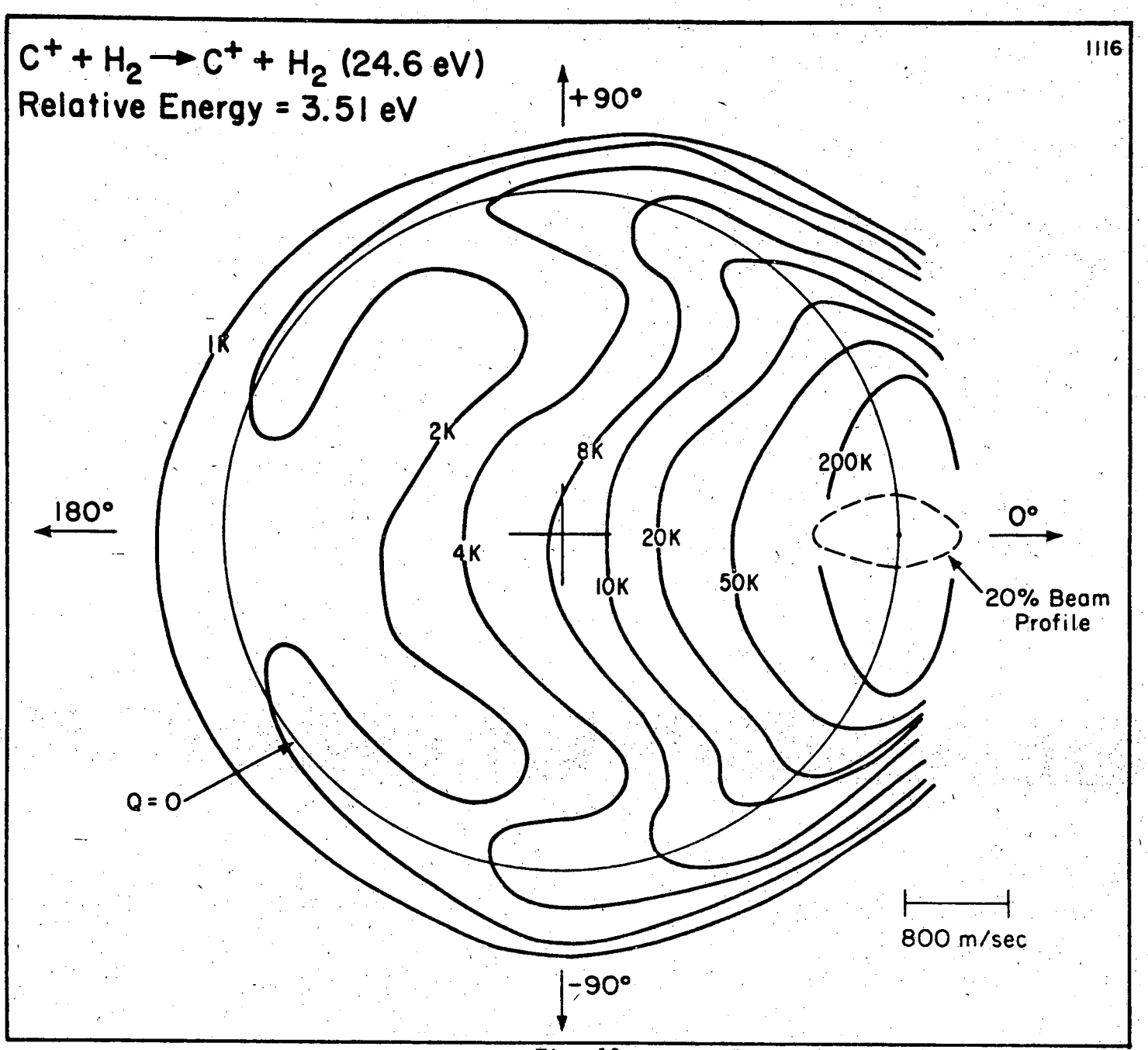


Fig. 13

XBL 739-1822

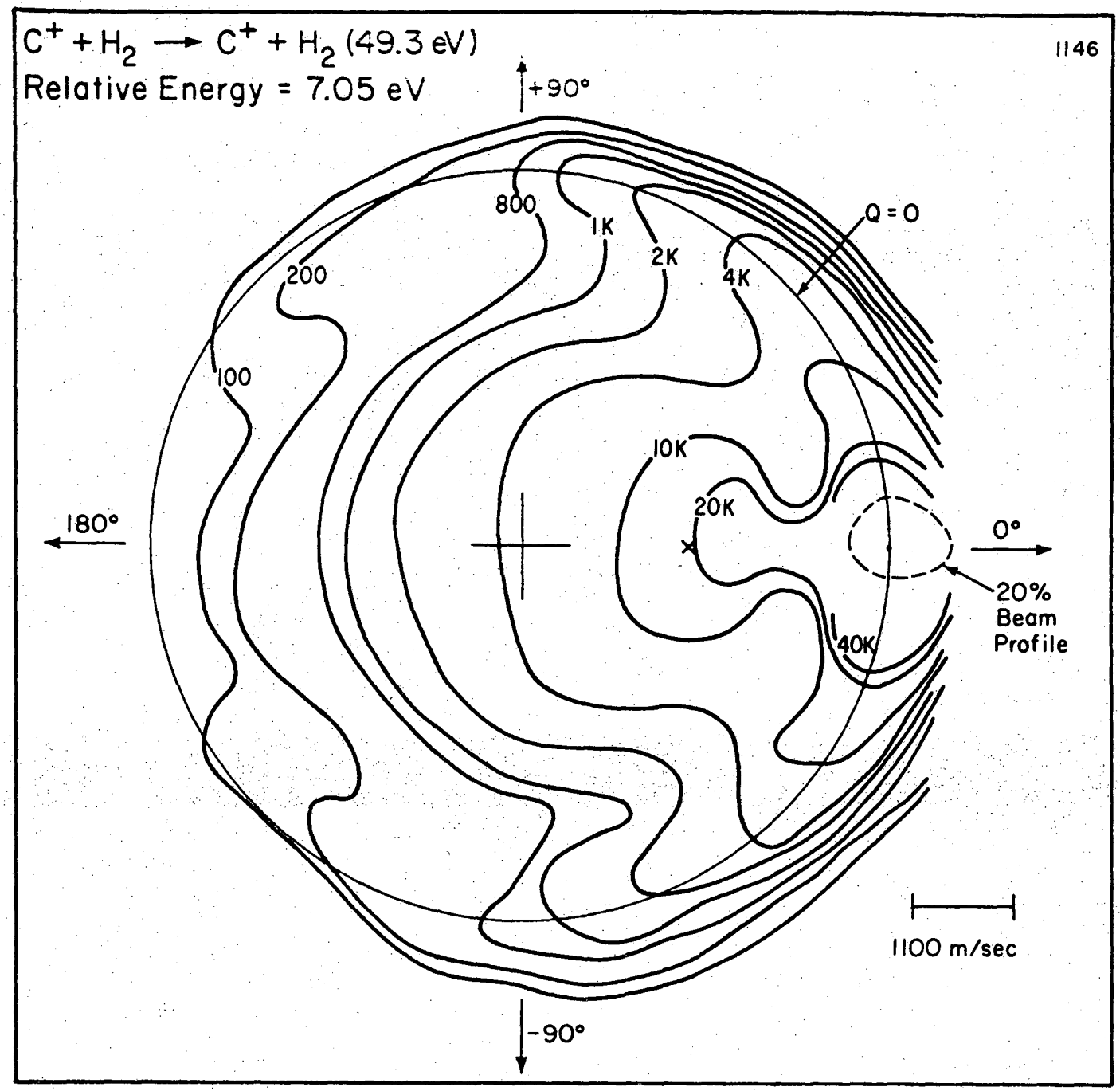


Fig. 14

XBL 739-1823

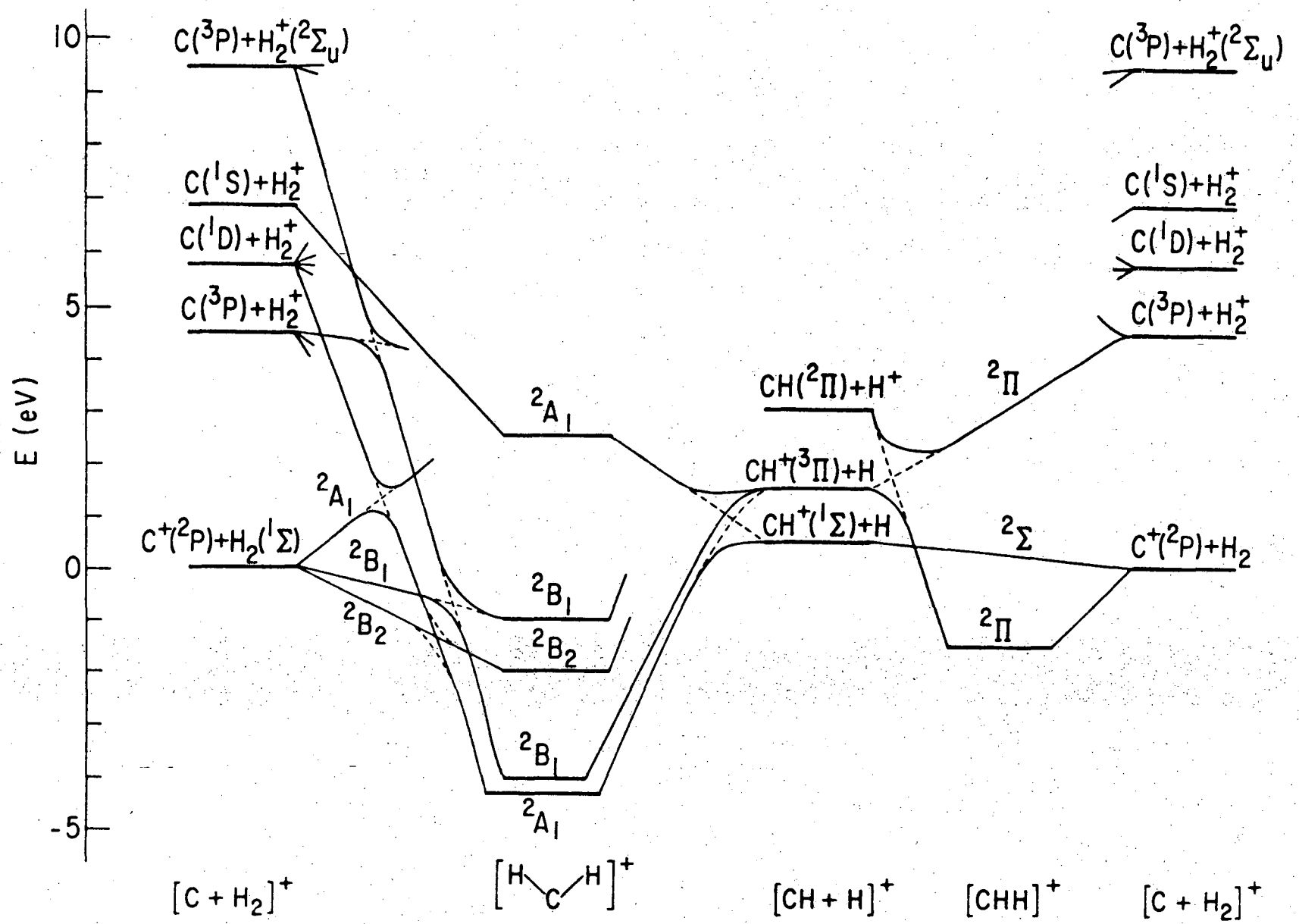


Fig. 15

XBL 737-6443

*TECHNICAL INFORMATION DIVISION*
*LAWRENCE BERKELEY LABORATORY*
*UNIVERSITY OF CALIFORNIA*
*BERKELEY, CALIFORNIA 94720*